NASA Technical Memorandum 79279

ASSESSMENT AT FULL SCALE OF EXHAUST NOZZLE-TO-WING SIZE ON STOL-OTW ACOUSTIC CHARACTERISTICS

U. von Glahn and D. Groesbeck
Lewis Research Center
Cleveland, Ohio

Prepared for the
Ninety-eighth Meeting of the Acoustical Society of America
Salt Lake City, Utah, November 26-30, 1979

ASSESSMENT AT FULL SCALE OF EXHAUST NOZZLE-TO-WING SIZE ON STOL-OTW ACOUSTIC CHARACTERISTICS

by U. von Glahn and D. Groesbeck

National Aeronautics and Space Administration
Lewis Research Center
Cleveland, Ohio 44135

E-215

ABSTRACT

On the basis of static aero/acoustic data obtained at model scale, the effect of exhaust nozzle size on flyover noise is evaluated at full scale for different STOL-OTW nozzle configurations. Three types of nozzles are evaluated: a circular/deflector nozzle mounted above the wing, a slot/deflector nozzle mounted on the wing, and a slot nozzle mounted on the wing. The nozzle exhaust plane location, measured from the wing leading edge was varied from 10 to 46 percent of the wing chord (flaps retracted). Flap angles of 20° (takeoff) and 60° (approach) are included in the study. Initially, perceived noise levels (PNL) are calculated as a function of flyover distance at 152 m altitude. From these plots static EPNL values, defined as flyover relative noise levels, then are obtained as functions of nozzle size for equal aerodynamic performance (lift and thrust). On the basis of these calculations, the acoustic benefits attributable to nozzle size relative to a given wing chord size are assessed.

INTRODUCTION

Advanced concepts for STOL aircraft often feature mounting the engines over the wing (OTW). One of the more commonly considered of these concepts is the use of slot or D-shaped nozzles mounted directly on the upper surface of the wing (fig. 1(a)). Another concept consists of using nozzles to which external flow deflectors are attached to vector the exhaust flow for attachment to the wing/flap surfaces. Representative configurations making use of external flow deflectors are shown in figures 1(b) and (c).

In reference 1, an assessment at full scale, based on model-scale data, was made of the effects associated with varying the nozzle/wing geometry on the OTW aeroacoustic characteristics. In references 2 to 5, acoustic data for the nozzle types shown in figure 1 are available at model scale for a fixed nozzle size with three wing chord sizes. For a selected wing chord size, these data, when properly scaled, provide nozzles (and associated flow deflectors) that differ in size by a factor of 2.25.

The present work is concerned with the effect of the exhaust nozzle size relative to a fixed wing chord size. In order to ascertain this effect, the thrust and lift values for the several nozzle concepts shown in figure 1 are maintained substantially constant by adjusting the jet exhaust velocity appropriately as the nozzle size is changed. A large nozzle implies the use of a turbofan engine. It is assumed herein that the single-stream, model-scale acoustic data also represent a turbofan engine in which the fan and core flows are completely mixed internally prior to the nozzle exhaust plane.

Through the use of increasingly larger nozzles and the associated lower jet velocities (to maintain a constant thrust value) the jet noise level is reduced by the usual term [20 log D + 10n log Uj]. (All symbols are defined in the nomenclature.) At the same time, however, the jet noise shielding benefit due to the wing is reduced by the decrease in the ratio of wing chord to nozzle size.

The purpose of this paper is to analyze, at full scale, the reduction in wing shielding benefits for jet noise associated with the use of increasingly larger sized nozzles for a fixed wing chord size. The three nozzle concepts illustrated in figure 1 are evaluated at full scale in terms of a flyover relative noise level, FRNL, (an equivalent static EPNL defined in ref. 1) at a flyover altitude of 152 m. Both approach and takeoff modes are considered. The noise evaluations are made for nozzle/wing configurations having substantially the same lift and thrust.

APPARATUS

Facilities

Aerodynamic data consisting of lift and thrust components were obtained using the test stand described in detail in references 1 and 2.

Acoustic data were taken in the flyover plane at an outdoor facility described in detail in references 1 and 3. The model-scale data were then scaled to full size by the appropriate scaling factors for size, flyover distance, and atmospheric attenuation. The full-scale flyover altitude was 152 m.

Model-Scale Nozzles

Slot. - The basic slot nozzles (ref. 3) used in this study consisted of the 5:1 nozzles shown in figure 2. These nozzles had equivalent diameters of 5.1 cm. The sidewall cutback angle, γ, was the same as the roof angle, β, for each respective nozzle.

Slot/deflector. - A 5:1 slot nozzle (fig. 3) was used with various external plate-type deflectors that turned the flow in order to promote flow attachment to the flap. Each of the nozzle sides converged at a 5° angle. The nominal dimensions of the nozzle at the

exhaust plane were 2.0 by 10.2 cm (equivalent diameter of 5.1 cm). Deflector dimensions of the configuration are summarized in the table given in figure 3.

Circular/deflector. - The conical nozzle (fig. 4) used in the study had a 5.2-cm exhaust diameter. Each flow deflector was held in place by two frames or "tracks" fastened to the nozzle. The deflector could be pivoted to various angles relative to the nozzle centerline. The inside bottom lip of the nozzle was located 0.1 chord (flaps retracted) above the surface of each wing. The nozzles were run at nominal cold-flow jet velocities of 195 and 260 m/s. A single nozzle configuration was also run at 145 m/s.

Model-Scale Wings

The model wings used in the studies are shown schematically in figure 5, together with pertinent dimensions. Details of their construction are given in reference 3. The wing chords with flaps retracted were 22.0, 33.0, and 49.5 cm. The wing models represent the upper surface contours of an airfoil with 20° (takeoff) and 60° (approach) deflected flaps.

ANALYSIS

Data Normalization

Lift and thrust characteristics. - All of the slot and slot/deflector nozzle configurations had weight flow losses as reported in reference 1. In order to make meaningful comparisons of the lift and thrust data, all the configurations are compared on the basis of equal weight flow. This was achieved by adjusting the measured static lift and thrust by the ratio of the ideal nozzle weight flow to the actual nozzle weight flow for each configuration tested. The adjusted lift and thrust were then ratioed to the ideal nozzle thrust giving the following expressions for the normalized lift and thrust:

$$\frac{L(W_i/W)}{T_i} \quad \text{and} \quad \frac{T(W_i/W)}{T_i}$$

All symbols are defined in the nomenclature.

Acoustics. - If the aerodynamic performance is normalized on an equal weight flow basis, the acoustic performance of the slot nozzles must also be normalized on an equal weight flow basis. In order to establish the necessary acoustic normalization, two additional slot nozzles (40° roof and sidewall cutback angles) of 16 and 30 percent greater area were tested with the 33 and 49.5 cm chord wings. This nozzle ($\beta = \gamma = 40^{\circ}$) was selected because it had the greatest weight flow loss. The 30-percent area increase was

required in order to have a measured weight flow equal to the calculated ideal flow of the initial nozzle in the presence of the wing (ref. 2). On the basis of these tests it was found that the increase in noise caused by increasing the nozzle area in proportion to the weight flow could be determined by the following empirical scaling relationship:

$$\Delta \text{ dB} = 10 \log (W_i/W)^{L_s/14}$$

The correction to the model-scale spectral data given by the preceding equation was applied to all the slot nozzle/wing data, both with and without an external deflector. No correction was necessary for the conical/deflector nozzle configuration data because weight flow losses were minimal or zero.

Scaling Procedure

Aerodynamic. - Initial acoustic work on the engine over-the-wing concept at NASA Lewis Research Center (1971) consisted of 1/13-scale model studies. The model-scale nozzles and mid-size wings used for the studies herein were part of these 1/13-scale studies. By selecting the mid-sized wing (33 cm chord) of the present wings as a base and a scale factor of 13:1, the full-scale wing chord (flaps retracted) used for the present study was 429 cm with a nominal effective nozzle diameter of 66 cm. By then scaling the smallest wing (22 cm chord) by a scale factor of 19.5:1, an effective nozzle diameter of 99 cm was obtained for the same 429 cm chord wing. Similarly, by scaling the largest wing (49.5 cm chord) by a scale factor of 8.67:1, an effective nozzle diameter of 44 cm was obtained for the same 429 cm chord wing.

Thrust is related to nozzle size and jet velocity by the term $D_{eff}^2 U_j^2$, where $D_{eff} = D_{act}\sqrt{W/W_i}$, so that for constant thrust, a change in jet velocity is associated with a change in nozzle size (diameter). It should be noted that the full-scale jet velocities herein vary by a factor of 1/2.25 for a range of effective nozzle diameters of 2.25. Thus, with a fixed wing chord size, the noise level for a constant thrust condition increases with increasing nozzle size and decreases with decreasing jet velocity.

The 260 m/s jet velocity used in the model-scale program was selected as the baseline jet exhaust velocity for the 66 cm effective diameter nozzles. On the basis of constant thrust, this gives calculated jet velocities of 390 m/s for the 44 cm effective diameter nozzles and 173 m/s for the 99 cm effective diameter nozzles. (For simplicity, no shock noise was assumed for the case of the 390 m/s jet velocity.)

Acoustic. - In order to obtain full-scale perceived noise levels, PNL, the model-scale noise spectra were scaled for size, distance, and atmospheric attenuation and frequency-shifted using the Strouhal relationship. From such full-scale spectra PNL

values were computed at a flyover height of 152 m for a standard day (288 K at 70% R.H.) These PNL values were computed at the model-scale test angles adjusted appropriately for the takeoff and approach attitudes shown in figure 6.

Typical plots of PNL as a function of flyover distance for a wing/flap configuration using a circular/deflector nozzle are shown in figure 7. From such plots of full-scale PNL values as a function of flyover distance (152 m altitude), a flyover relative noise level (FRNL) was computed as described in appendix A of reference 1. The term "relative" is used herein since the conventional definition of effective perceived noise level (EPNL) includes forward flight effects, whereas the present data are for static conditions. The omission of flight effects, however, does not significantly affect the present flyover relative noise level comparisons between the various configurations. Comparisons of relative flyover noise level of the various nozzle/wing configurations then were made at as nearly equal magnitudes of lift and thrust as possible.

Jet velocity exponents at each radiation angle were determined for the full-scale PNL (n_p) values and the FRNL (n_F) values with jet exhaust velocity, as described in appendix A.

Once the n_p and n_F values were determined from the model-scale test conditions, (U_j = 195 and 260 m/s), the PNL and FRNL values at constant thrust were calculated for the jet velocities associated with the 44 and 99 cm effective diameter nozzles (390 and 173 m/s, respectively) as follows:

$$PNL = PNL_{BASE} + 10\, n_p \log U_j/U_{j,BASE}$$

where the subscript BASE refers to the PNL for each full-scale nozzle with a jet velocity of 260 m/sec ($U_{j,BASE}$) and a wing chord of 429 cm.

Similarly, the FRNL values at constant thrust are calculated as follows:

$$FRNL = FRNL_{BASE} + 10\, n_F \log U_j/U_{j,BASE}$$

where the subscript BASE refers to the FRNL for each full-scale nozzle, again with a jet velocity of 260 m/s and a wing chord of 429 cm.

Configuration Selections

In order to compare the noise levels of the various nozzle/wing configurations, the lift and thrust characteristics of the configurations should be substantially the same. For the most part the lift and thrust values given in references 2 to 5 were used to select such aerodynamically similar configurations for both approach and takeoff modes.

Where such data were lacking additional measurements were made on the aerodynamic facility using the procedures described in references 2 and 4.

From a practical point of view, nozzles with short deflectors (in the axial direction) are more desirable than long ones because of less weight and fewer stowage problems for cruise considerations. With short deflectors, however, steeper deflector angles are needed compared to those for long deflectors in order to promote good jet exhaust flow attachment to the flap and give high lift augmentation (refs. 2 to 5). Once the flow is attached to the flap, the lift and thrust components for short and long flaps are generally similar, with a slight favoring of the short deflectors for the takeoff mode and the long deflectors for the approach mode. Herein, only the short deflectors used with the circular and slot nozzles (refs. 1 to 5) will be included. The specific model-scale dimensions of the deflectors used with the slot and circular nozzles are given in figures 3 and 4, respectively.

For roof-angled slot nozzles without external deflectors, those with nozzle sidewall cutback provide somewhat better jet exhaust flow attachment for high flap angles (approach mode) than those without sidewall cutback (ref. 2). Consequently, only the data for slot/cutback nozzle configurations are included herein.

The lift/thrust characteristics for the takeoff and approach modes are shown in figures 8 to 10 for circular/deflector, slot/deflector, and slot/cutback nozzle configurations. From these data, configurations that yield substantially equal lift and thrust measurements were identified (solid symbols) for the acoustic analysis herein. The selected nozzle roof/deflector angles are summarized in the following table:

Operational mode	Nozzle	Roof/sidewall angle, deg	Deflector angle, deg
Takeoff (20° flap)	Circular/deflector	--	25
	Slot/deflector	--	20
	Slot/cutback	30	--
Approach (60° flap)	Circular/deflector	--	30
	Slot/deflector	--	25
	Slot/cutback	40	--

It is obvious from figures 8 to 10, that other nozzle configurations could have been selected in some instances than those identified in the preceding table. For example, a slot/cutback nozzle with a 20° roof angle (figs. 8(a) and (b)) has a larger thrust component but a slightly smaller lift component than the selected nozzle with a 30° roof angle. However, experience has shown that jet flows from nozzles with low roof or deflector angles frequently are sensitive to flow separation from the flap. In particular, this

sensitivity to flow separation can become very apparent in flight. On this basis, the nozzle with the 30° roof angle was selected herein for the acoustic comparisons. (It should be noted that the noise levels were nearly identical for the preceding two nozzle/wing configurations (ref. 1).)

PERCEIVED NOISE LEVEL

In this section, data will be shown to illustrate PNL trends with variations in nozzle size for constant thrust and wing chord size and for several nozzle chord locations.

Representative variations of PNL with nozzle size (at constant thrust) are shown in figure 11 for circular/deflector and slot/cutback nozzles. Both nozzles were located at 21 percent chord for the takeoff mode (20° flap deployment). Because an increase in nozzle size (D_{eff}^2) is accompanied by a decrease in jet velocity for constant thrust conditions, the PNL values decrease with an increase in nozzle size. The peak PNL values occur near a radiation angle of 110° with the circular/deflector nozzle, while those for the slot/cutback nozzle occur near 90°. In general, however, the PNL variation with radiation angles were similar for both nozzle concepts.

Similar PNL trends with nozzle size were obtained in the approach mode (60° flap deployment) as shown in figure 12. In the approach mode, however, a significant amount of deflector associated noise was measured in the forward quadrant with the circular/deflector nozzle configuration. This is more clearly shown in figure 13 in which the PNL values obtained with the circular/deflector nozzle are compared directly with those for the slot/cutback nozzle. The PNL with the slot/cutback nozzle peaks near a radiation angle of 90° while that with the circular/deflector nozzle peaks in the range of 50° to 70°. In this latter angular range, the PNL with the circular/deflector nozzle is 7 dB greater, due to deflector noise, than that with the slot/cutback nozzle.

The typical effect on PNL of chordwise location of the nozzle relative to the wing leading edge is shown in figure 14 for the takeoff mode.

The PNL increases with increasing chordwise location of the nozzle. This is a result of reducing the length of acoustic shielding of the wing/flap system to the jet noise. Similar trends were observed for nozzle sizes other than those used in figure 14 and also for the approach mode.

FLYOVER RELATIVE NOISE LEVEL

From PNL plots such as shown in figures 11 to 14, FRNL values were calculated for each nozzle/wing combination by the method described in reference 1.

Effect of Nozzle Size

For constant thrust, the FRNL decreases with increasing nozzle size, as shown in figures 15 and 16 for the takeoff and approach modes, respectively. This is primarily due to the reduced jet velocity associated with the constant thrust condition. The reduction in FRNL, due to a lower jet velocity, is partly offset by the increase in nozzle size as well as a decrease in effective shielding of the jet noise. The latter is a function of the ratio of nozzle size to wing/flap shielding length. Thus, the shielding benefits with a fixed wing chord size and nozzle chord location are reduced with increasing nozzle size.

In the takeoff mode (fig. 15), the slot/cutback nozzle yields the highest FRNL values at a given nozzle chord location, while the slot/deflector nozzle yields the lowest FRNL values. The difference between these FRNL values at 21 percent chord is 3 dB, with the circular/deflector nozzle about mid-way between the values for the other two nozzles.

In the approach mode (fig. 16), the slot/deflector and slot/cutback nozzles generally yielded lower FRNL values than those for the circular/deflector nozzle. The FRNL differences between the slot- and circular-type nozzles vary as a function of nozzle size and nozzle chord location as indicated by the data in figure 16.

The ranges of data shown in figures 15 and 16 are plotted together in figure 17 in order to provide a comparison of the FRNL values between the takeoff and approach modes. It is apparent that the FRNL values for the takeoff mode are significantly higher than those for the approach mode. The largest overall FRNL differences between the takeoff and approach modes occurs with the largest nozzle (99 cm) and amounts to about 8 dB. The largest difference in FRNL values for a given nozzle/wing configuration amounts to about 6 dB and occurred in the approach mode.

Effect of Nozzle Chord Location

The effect of nozzle chord location is illustrated in figures 18 and 19 for the takeoff and approach modes, respectively.

In the takeoff mode (fig. 18), the highest FRNL values generally are obtained with the nozzle at 46 percent chord because the wing/flap shielding length is the shortest of those included in this study. With the nozzles located at 21 percent chord, the FRNL values are lower compared to those obtained with the nozzle at 46 percent chord. The reduction in FRNL is caused by the greater jet noise shielding surface downstream of the nozzle exhaust plane when the nozzles are located at 21 percent chord compared to the 46 percent nozzle chord location. When the nozzles are located at 10 percent of chord, the jet noise sources are provided an inadequate shielding length in the forward

arc. Consequently, even though the aft shielding surface is increased, jet and deflector noise "leakage" around the wing leading edge can increase the FRNL values at the 10-percent nozzle chord location compared with the 21-percent chord nozzle location (data for 44 cm diameter nozzle).

In the approach mode (fig. 19) similar trends with nozzle chord location as those discussed for the takeoff mode were obtained. It should be noted that for the approach mode, the FRNL values for the 10-percent nozzle chord location increased, relative to the 21-percent location, for both the 44- and 66-cm diameter nozzles whereas this trend was only observed with the 44-cm diameter nozzle for the takeoff mode. The cause for this increase again is believed to be insufficient wing shielding upstream of the jet and deflector noise sources.

CONCLUDING REMARKS

The analyses and results obtained herein indicate that in terms of flyover relative noise levels (an equivalent of static EPNL) for engine over-the-wing type aircraft the noise levels are less during approach than during takeoff by up to 8.0 dB. With a constant wing size, increasing the nozzle size and decreasing the jet velocity, in order to maintain constant thrust, reduces the overall noise levels but also reduces the shielding benefits of the wing/flap system. In general, the FRNL values are decreased by moving the nozzle from 46 to 10 percent chord. This is due to the increased wing/flap jet noise shielding length with the forward nozzle placement. Finally, when an external deflector is used to promote jet flow attachment to the flap during approach, the deflector can become the dominant noise source.

NOMENCLATURE

A, B, C, X, Y, y	local component dimensions
D	diameter
D_{act}	geometric equivalent diameter required for equal mass flow
D_{eff}	effective diameter defined by $D_{act}\sqrt{W/W_i}$
EPNL	effective perceived noise level
FRNL	flyover relative noise level
L	measured lift

L_f	projected surface distance from nozzle exit plane to wing leading edge (see (fig. 5)
L_p	projected surface distance (see fig. 5)
L_s	surface distance measured from nozzle exit plane to flap trailing edge (see fig. 5)
ℓ	deflector lip chord
ℓ_T	distance from nozzle exit to deflector trailing edge (see fig. 3)
n	velocity exponent
n_p	velocity exponent for PNL
n_F	velocity exponent for FRNL
PNL	perceived noise level
T	measured thrust
T_i	ideal thrust
U_j	jet exhaust velocity
W	measured weight flow
W_i	ideal weight flow
α	flap angle
β	roof/deflector angle
γ	nozzle sidewall cutback angle
θ	aircraft attitude corrected noise radiation angle

Subscripts:

BASE	refers to PNL for each full-scale nozzle at U_j = 260 m/s and wing chord of 429 cm
1, 2	measured values

APPENDIX A

VELOCITY EXPONENTS

Jet velocity exponents were determined at each radiation angle using the full-scale PNL values for each nozzle/wing configuration at the test jet velocities as follows:

$$n_p = \frac{PNL_2 - PNL_1}{10 \log \left(U_{j,2} / U_{j,1} \right)}$$

In figure A1 the variation of PNL with directivity angle, θ, is shown for jet velocities of 145, 195, and 260 m/s. These data are for a circular/deflector nozzle (30° deflector angle) with a 66-cm effective diameter and a wing chord of 429 cm in the takeoff mode (20° flap deflection). On the basis of the preceding equation, the jet velocity exponents, n_p, for these data are tabulated in the following table:

Velocity ratio	n_p \ θ	10°	30°	50°	70°	80°	90°	110°	130°
260/195		7.7	8.2	8.2	9.1	9.5	10.0	8.2	5.4
260/145		7.6	7.4	7.6	8.6	9.4	9.8	9.2	6.4
195/145		7.5	7.1	7.1	8.2	9.4	9.7	9.7	7.8
Average	n_p	7.6	7.6	7.6	8.6	9.4	9.8	9.2	6.5

The value of n_p for all other nozzle/wing configurations was obtained in the same manner except that the exponent was based on jet velocities of 195 and 260 m/s.

In a similar manner, a jet velocity exponent, n_F, was determined for the flyover relative noise level, FRNL. The value of n_F was calculated by the following equation:

$$n_F = \frac{FRNL_2 - FRNL_1}{10 \log \left(U_{j,2} / U_{j,1} \right)}$$

For the nozzle/wing configuration used in the preceding PNL example, the following n_F values for the variation of FRNL with jet velocity were obtained:

Velocity ratio, $U_{j,2}/U_{j,1}$	n_F
260/195	8.33
260/145	8.23
195/145	8.15
Average n_F	8.24

Representative n_p-values are shown in figures A2 and A3 for the takeoff and approach modes, respectively, as a function of flyover distance (radiation angle) in order to illustrate the variation in n_p with nozzle configuration, nozzle size, and operational mode (flap angle) for a fixed wing chord size. The values shown by the curves are averages of all nozzle chord locations and nozzle roof/deflector angles used herein. In general, the n_p-values for the takeoff attitude tend to be lower in the forward quadrant than those for the approach attitude (n_p ~7-8 compared with n_p ~8-9, respectively).

The velocity exponents for the flyover relative noise levels, n_F, are summarized in Table I. The FRNL velocity exponent, n_F, is seen to vary from 7 to 10, except when the nozzle deflector noise is the dominant noise source. In the latter case the exponent is of the order of 5 to 6.

REFERENCES

1. D. Groesbeck and U. von Glahn, "Assessment at Full Scale of Nozzle/Wing Geometry Effects on OTW Aeroacoustic Characteristics," NASA TM-79168 (1979).

2. U. von Glahn and D. Groesbeck, "Nozzle and Wing Geometry Effects on OTW Aerodynamic Characteristics," NASA TM X-73420 (1976).

3. U. von Glahn and D. Groesbeck, "Geometry Effects on STOL Engine-Over-the-Wing Acoustics with 5:1 Slot Nozzles," NASA TM X-71820 (1975).

4. U. von Glahn and D. Groesbeck, "OTW Noise Correlation for Several Nozzle Wing Geometries Using a 5:1 Slot Nozzle with External Deflectors," NASA TM X-73529 (1976).

5. U. von Glahn and D. Groesbeck, "Effect of External Jet-Flow Deflector Geometry on OTW Aero-Acoustic Characteristics," NASA TM X-73460 (1976).

TABLE I. - VELOCITY EXPONENTS

(a) Takeoff mode (20^{o} flap angle)

Nozzle effective diameter, cm	Nozzle	Percent chord	Deflector length, cm	FRNL velocity exponent, n_F			
				Roof/deflector angle, β, deg			
				20	25	30	40
99.0	Slot/cutback	21	----	7.9	---	8.3	8.9
		46	----	7.2	---	7.7	8.4
66.0	Circular/deflector	10	53.8	---	8.2	8.3	----
		21	53.8	---	9.1	8.3	----
	Slot/cutback	21	----	7.6	---	9.0	8.4
		46	----	3.3	---	8.0	8.0
	Slot/deflector	21	8.3	9.1	8.6	9.0	8.2
		46	8.3	9.0	---	8.1	8.4
44.0	Circular/deflector	10	35.9	---	8.3	7.9	----
		21	35.9	---	8.4	7.8	----
	Slot/cutback	21	----	9.7	---	9.6	----

(b) Approach mode (60^{o} flap angle)

99.0	Slot/cutback	21	----	8.5	---	8.6	8.1
		46	----	8.5	---	8.8	8.7
66.0	Circular/deflector	10	53.8	---	---	8.2	5.4*
		21	53.8	---	---	8.0	5.7*
	Slot/cutback	21	----	---	---	9.5	9.4
		46	----	---	---	9.5	8.9
	Slot/deflector	21	8.3	---	8.5	9.0	8.3
		46	8.3	8.7	9.0	8.6	8.9
44.0	Circular/deflector	10	35.9	---	8.3	7.7	----
		21	35.9	---	8.2	8.2	----
	Slot/cutback	21	----	---	---	---	7.0

*Deflector dominated noise.

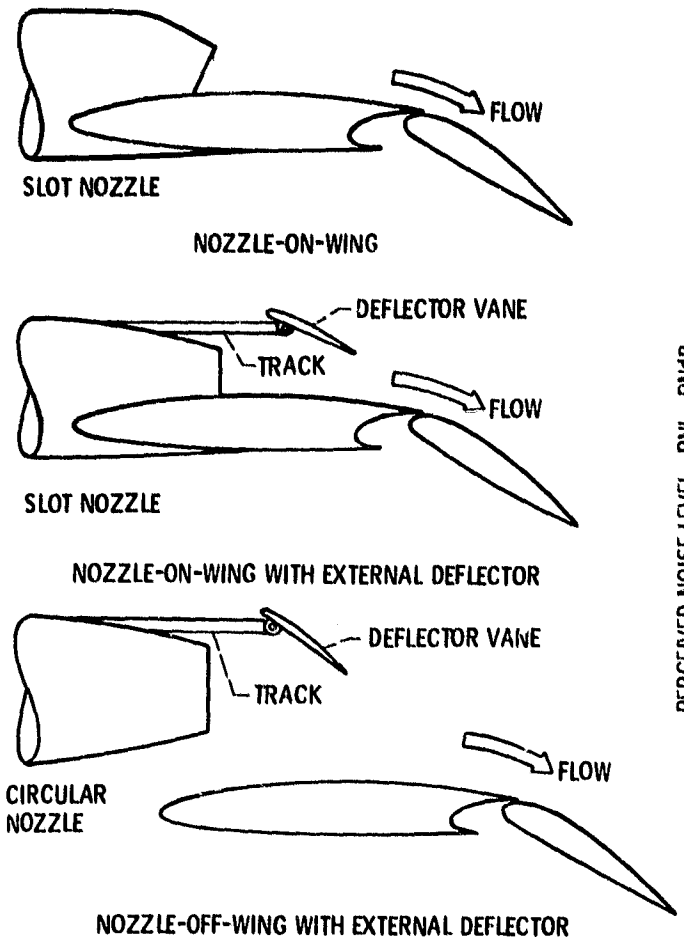

Figure 1. - Conceptual OTW nozzle/wing configurations.

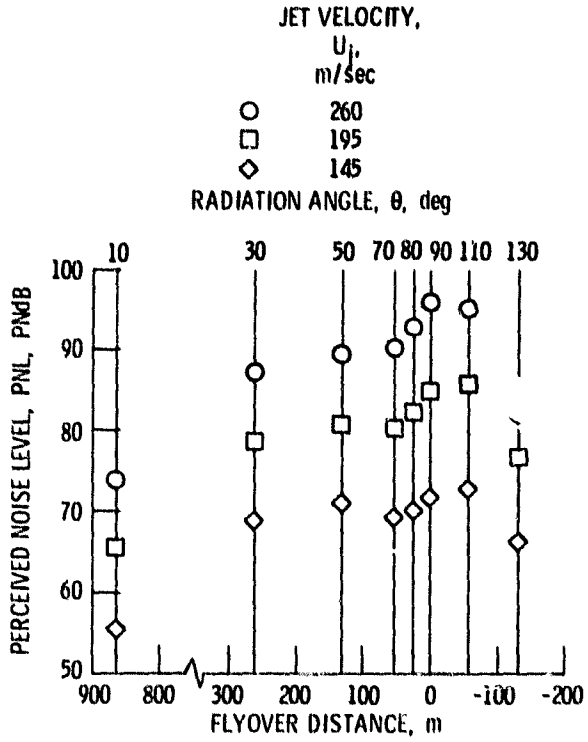

Figure A1. - Typical effect of jet velocity on PNL. Circular/deflector nozzle; takeoff mode; 30^0 deflector angle (β); nozzle at 21% chord; effective nozzle diam., D_{eff}, 66 cm.

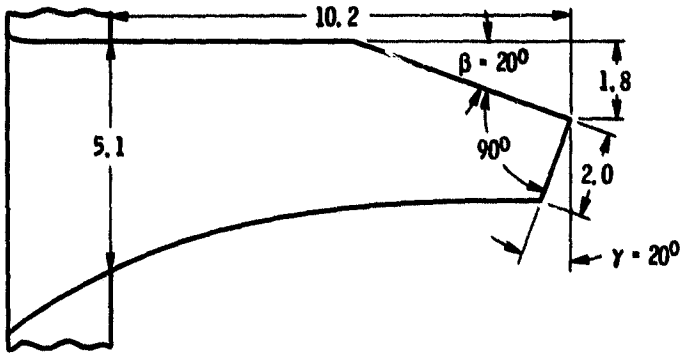

(a) 20° ROOF ANGLE NOZZLE.

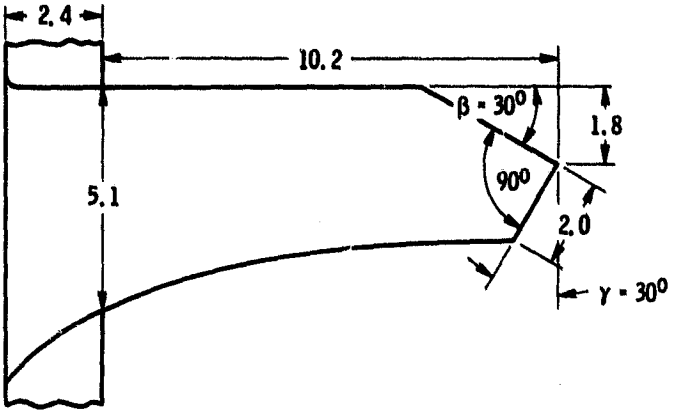

(b) 30° ROOF ANGLE NOZZLE.

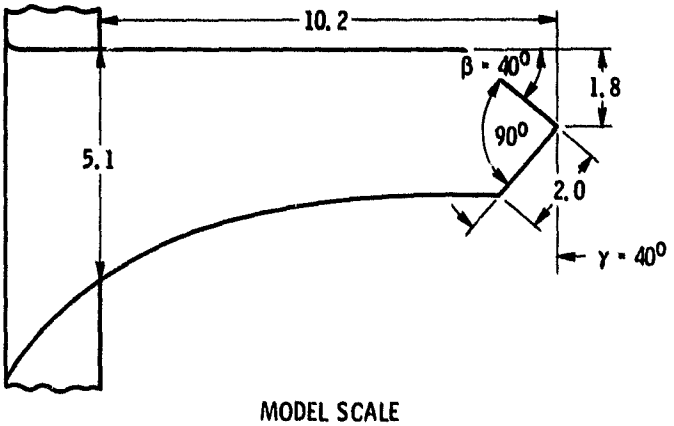

MODEL SCALE

(c) 40° ROOF ANGLE NOZZLE.

Figure 2. - Sketches of model scale slot nozzles with sidewall cutback. Dimensions in centimeters. All nozzles 10.2 centimeters wide.

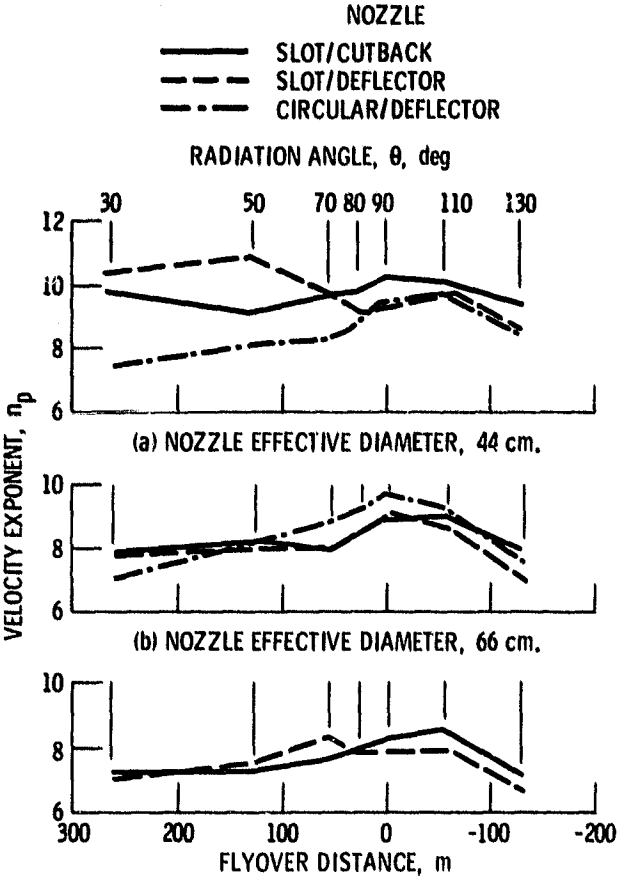

Figure A2. - Variation of average velocity exponent, n_p, with flyover distance for several nozzle configurations and sizes with fixed wing chord size (429 cm). Takeoff mode.

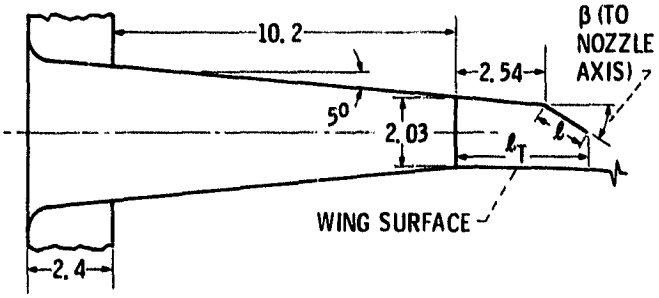

DEFLECTOR ANGLE, β, deg	DEFLECTOR LIP, ℓ, cm	TOTAL DEFLECTOR LENGTH ℓ_T, cm
40	0.64	3.25
30	↓	3.25
25		3.30
20		3.35

Figure 3. - Sketch of model scale 5:1 slot/deflector nozzle. Dimensions in centimeters. All deflectors were 15.2 cm wide. Nozzle width is 10.2 cm. Reference 1.

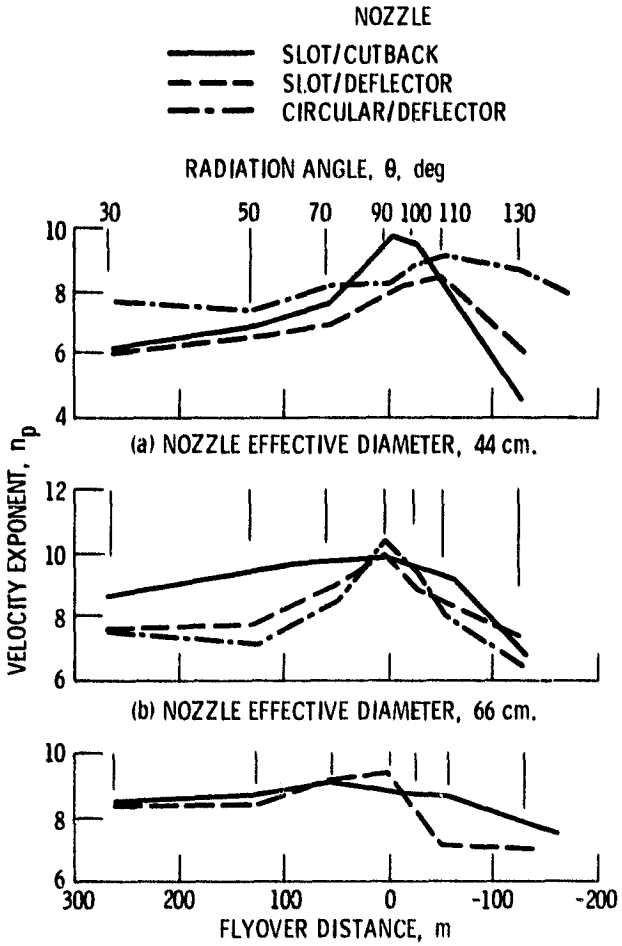

(a) NOZZLE EFFECTIVE DIAMETER, 44 cm.

(b) NOZZLE EFFECTIVE DIAMETER, 66 cm.

(c) NOZZLE EFFECTIVE DIAMETER, 99 cm.

Figure A3. - Variation of average velocity exponent, n_p, with flyover distance for several nozzle configurations and sizes with fixed wing chord size (429 cm). Approach mode.

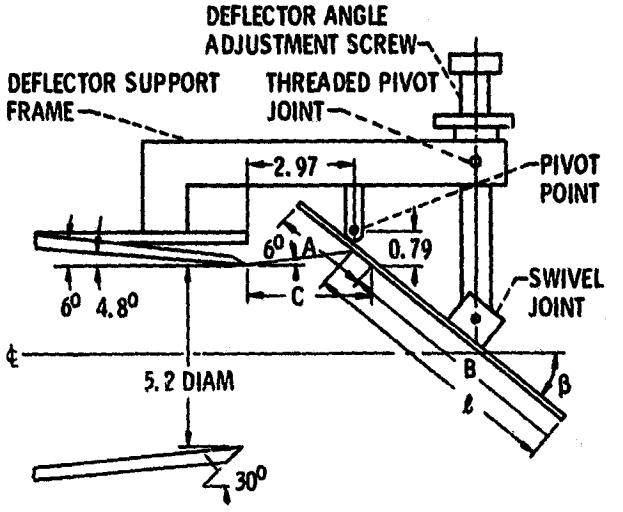

ℓ	A	B	C	β
4.14	2.51	3.18	3.91	20°
	2.29	3.40	3.66	25°
	2.18	3.51	3.51	30°
	2.06	3.63	3.25	40°

Figure 4. - Schematic sketch of model scale circular nozzle and flow deflectors. Dimensions in centimeters.

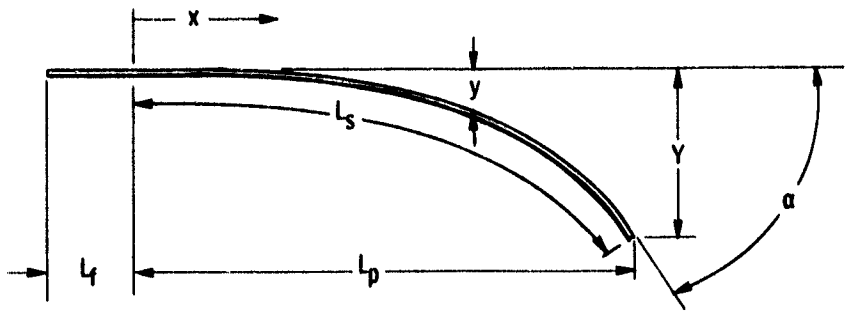

WING COORDINATES

FLAP ANGLE, α, deg	WING CONFIGURATION	x/L_p / y/Y	0-0.4	0.5	0.6	0.7	0.8	0.9	0.95	0.975	1.0
20	22 AND 33 cm CHORD		0	0.04	0.13	0.26	0.44	0.70	0.85	-----	1.0
	49.5 cm CHORD		0	0.025	0.10	0.225	0.42	0.70	0.85	-----	1.0
60	ALL		0	0.02	0.055	0.125	0.24	0.44	0.61	0.76	1.0

WING DIMENSIONS

FLAP ANGLE, α, deg	WING SIZE (FLAPS RETRACTED), cm	NOZZLE LOCATION, % CHORD	Y, cm	L_f, cm	L_p, cm	L_s, cm
20	22.0	21	4.4	4.6	22.5	23.3
		46		10.2	16.9	17.8
	33.0	10	6.6	3.3	37.4	39.0
		21		6.9	33.8	35.4
		46		15.2	25.4	27.0
	49.5	10	10.2	5.0	56.0	58.4
		21		10.2	50.8	53.2
		46		22.9	38.1	40.6
60	22.0	21	9.6	4.6	20.3	25.7
		46		10.2	14.7	20.3
	33.0	10	14.3	3.3	34.1	42.3
		21		6.9	30.5	38.7
		46		15.2	22.1	30.2
	49.5	10	21.5	5.0	50.9	62.8
		21		10.2	45.7	57.6
		46		22.9	33.1	45.1

Figure 5. - Model-scale wing dimensions and coordinates. Dimensions in centimeters.

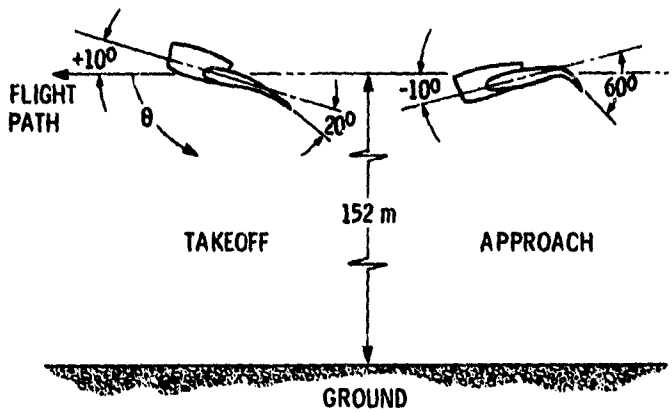

Figure 6. - Schematic of nozzle/wing orientation used for configuration aeroacoustic comparisons.

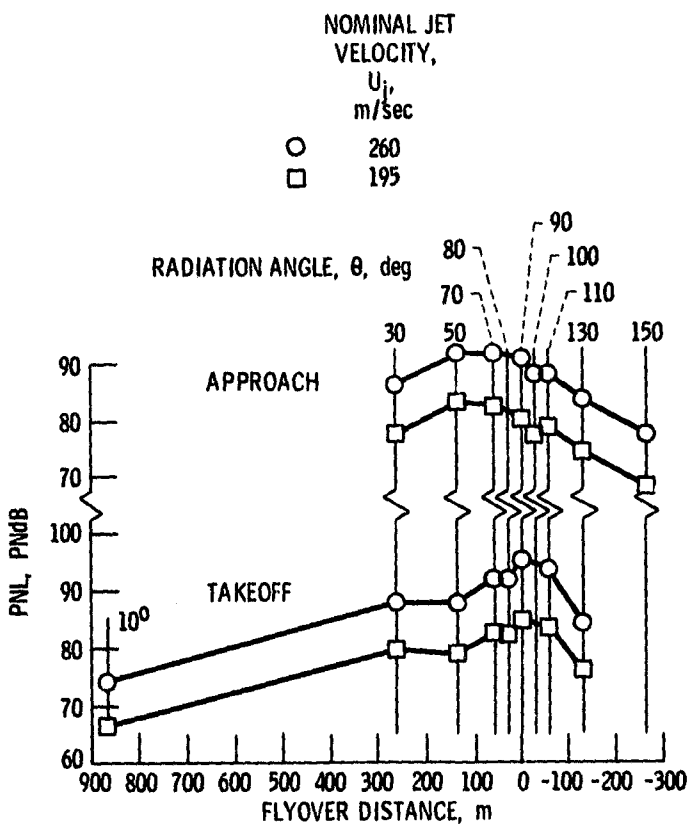

Figure 7. - Typical PNL variations with flyover distance. Circular/deflector nozzle; deflector length, 53.8 cm; deflector angle, β, 30°; 429 cm chord wing; nozzle at 10% chord; 152 m altitude.

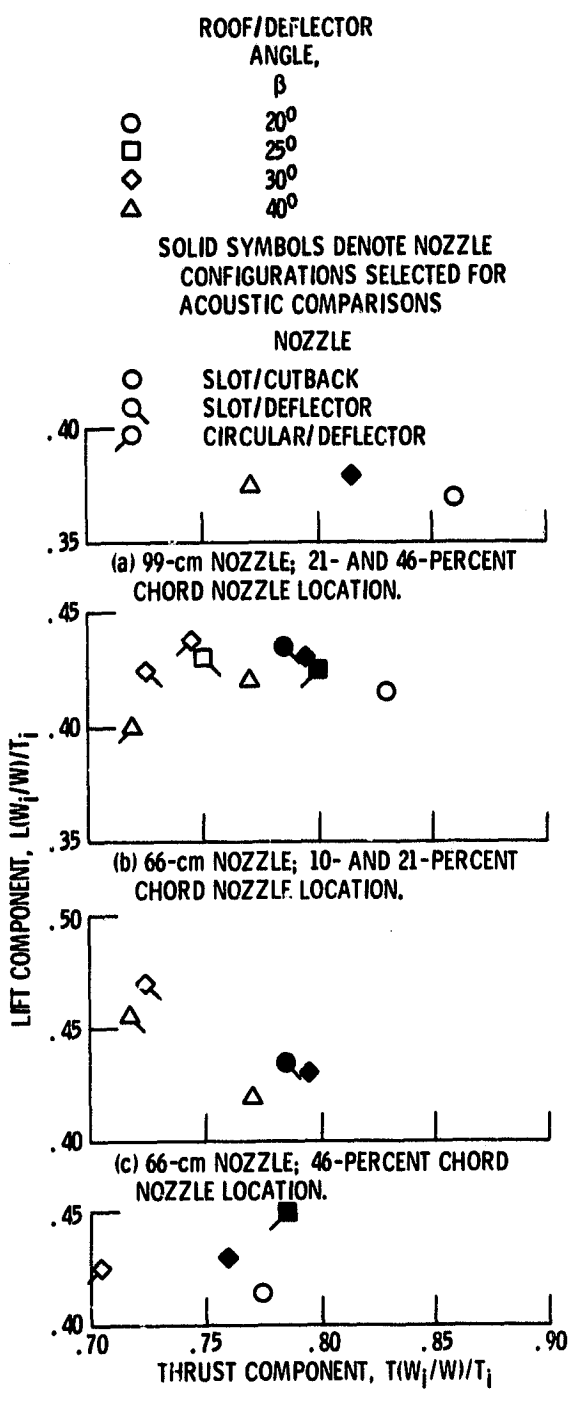

(a) 99-cm NOZZLE; 21- AND 46-PERCENT CHORD NOZZLE LOCATION.

(b) 66-cm NOZZLE; 10- AND 21-PERCENT CHORD NOZZLE LOCATION.

(c) 66-cm NOZZLE; 46-PERCENT CHORD NOZZLE LOCATION.

(d) 44-cm NOZZLE; 10- AND 21-PERCENT CHORD NOZZLE LOCATION.

Figure 8. - Takeoff mode aerodynamic characteristics.

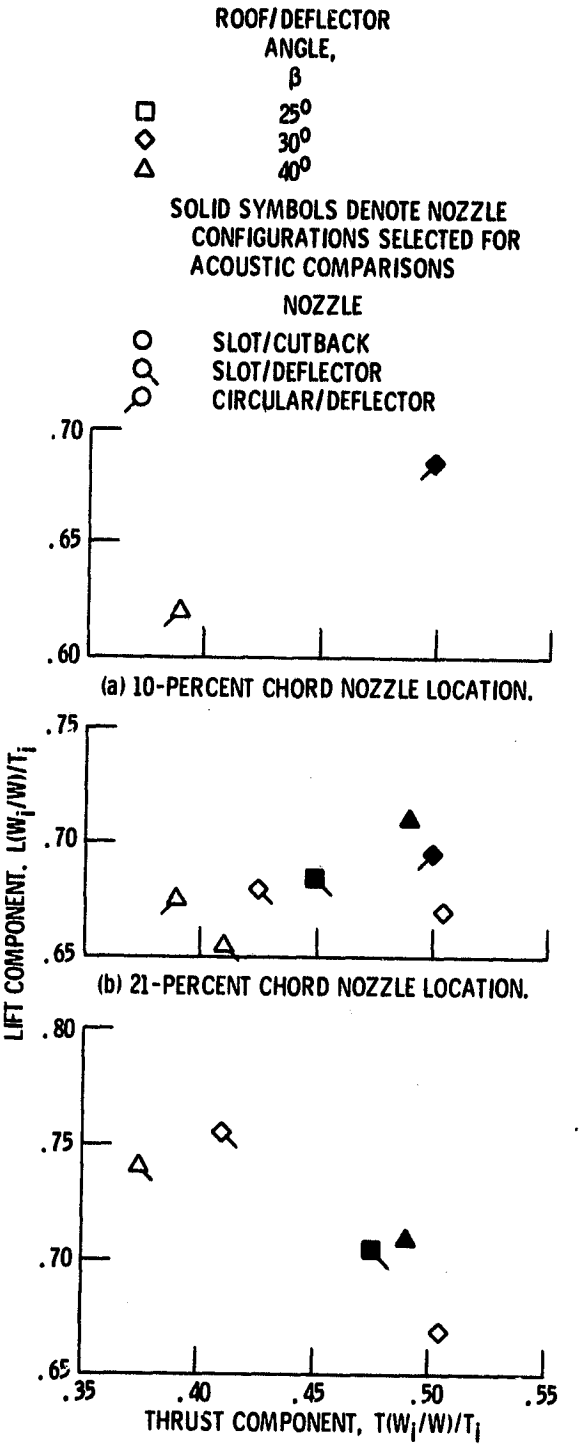

(a) 10-PERCENT CHORD NOZZLE LOCATION.

(b) 21-PERCENT CHORD NOZZLE LOCATION.

(c) 46-PERCENT CHORD NOZZLE LOCATION.

Figure 9. - Approach mode aerodynamic characteristics. 66 cm nozzle.

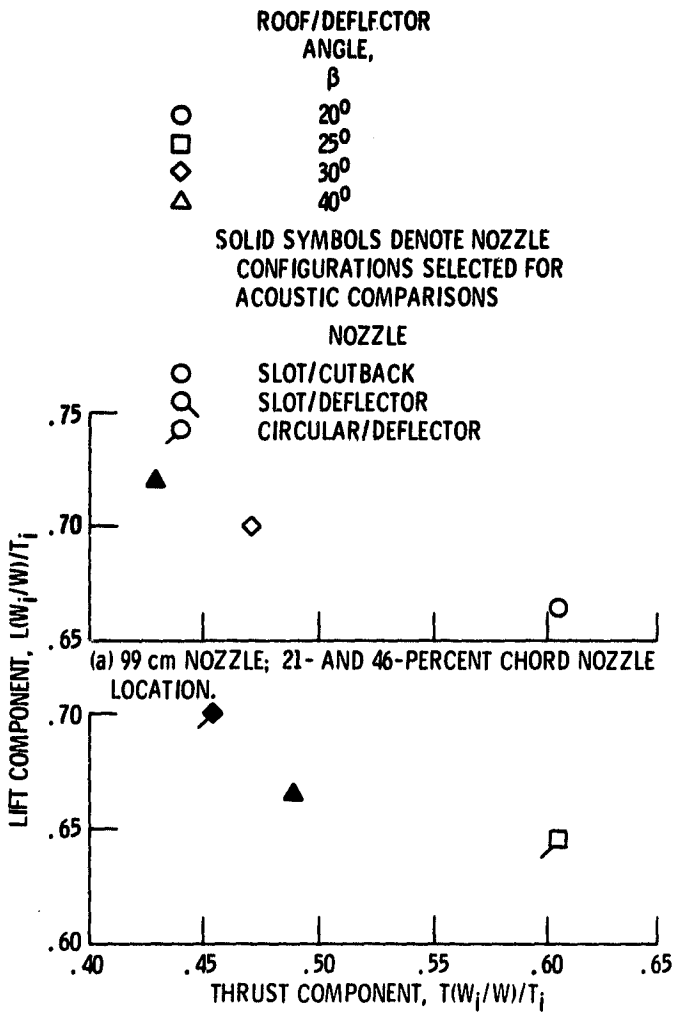

(a) 99 cm NOZZLE; 21- AND 46-PERCENT CHORD NOZZLE LOCATION.

(b) 44 cm NOZZLE; 10- AND 21-PERCENT CHORD NOZZLE LOCATION.

Figure 10. - Approach mode aerodynamic characteristics.

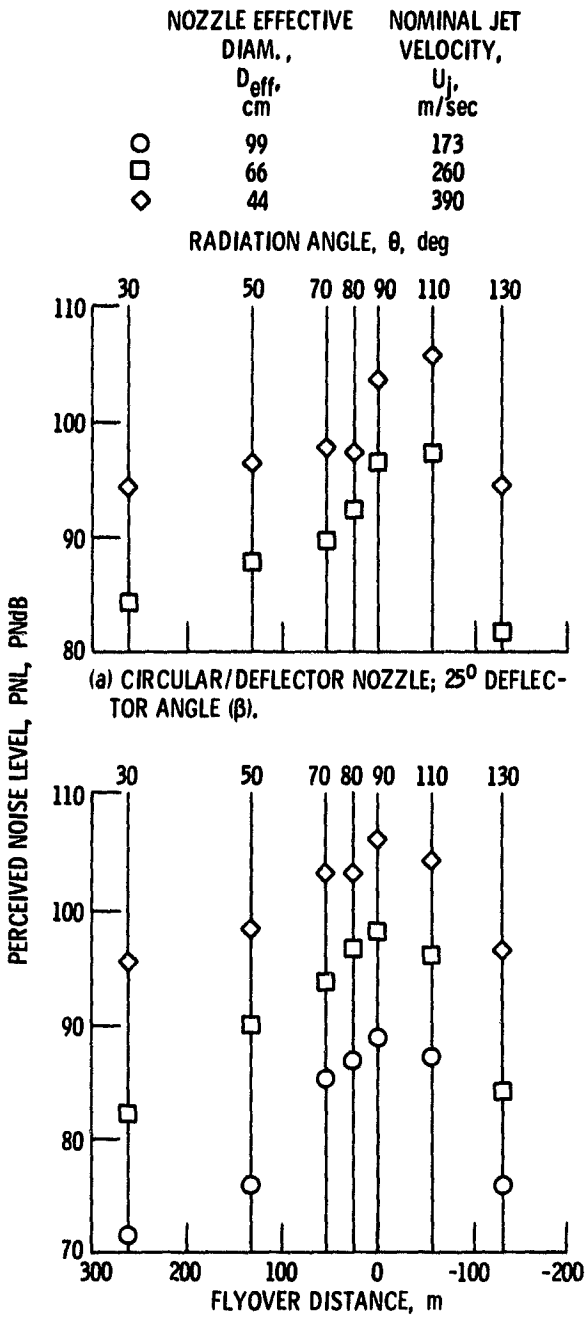

(a) CIRCULAR/DEFLECTOR NOZZLE; 25° DEFLECTOR ANGLE (β).

(b) SLOT/CUTBACK NOZZLE; 30° ROOF ANGLE (β).

Figure 11. - Typical PNL variations with flyover distance for takeoff mode. Nozzles at 21% chord.

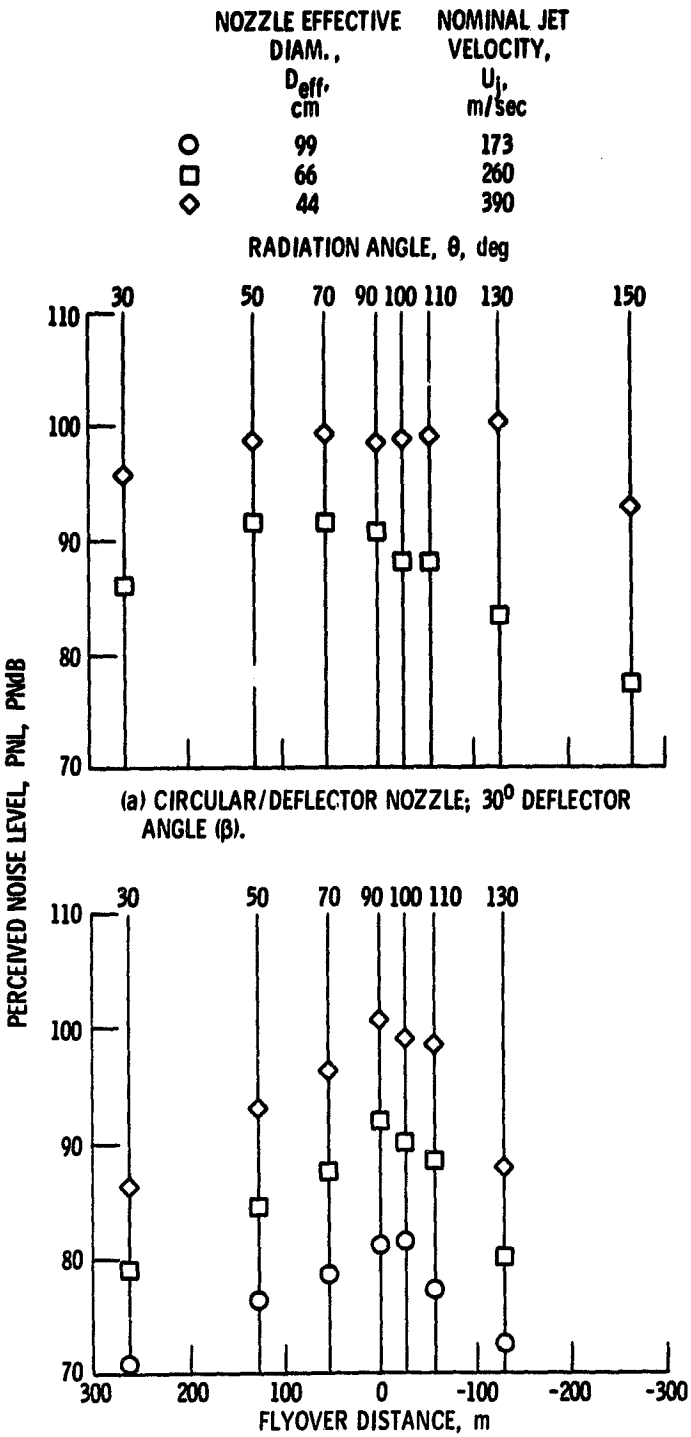

Figure 12. - Typical PNL variations with flyover distance for approach mode. Nozzles at 21% chord.

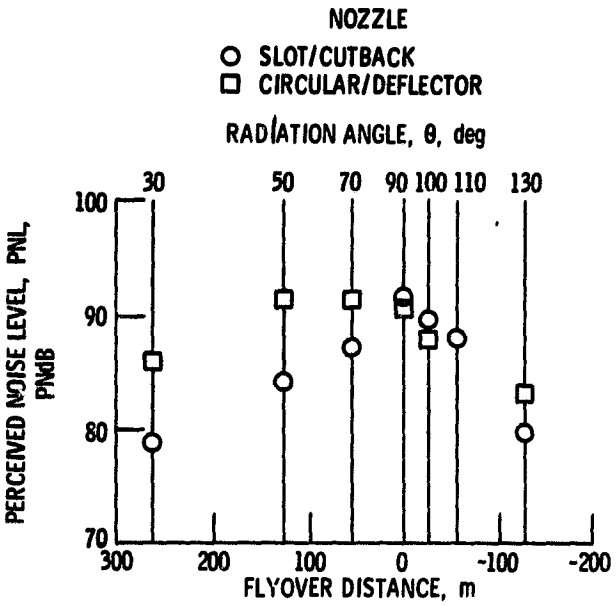

Figure 13. - PNL comparison of circular/deflector nozzle and slot/cutback nozzle with wing in approach mode. Nozzles at 21% chord; nozzle effective diam., D_{eff}, 66 cm; jet velocity, U_j, 260 m/sec.

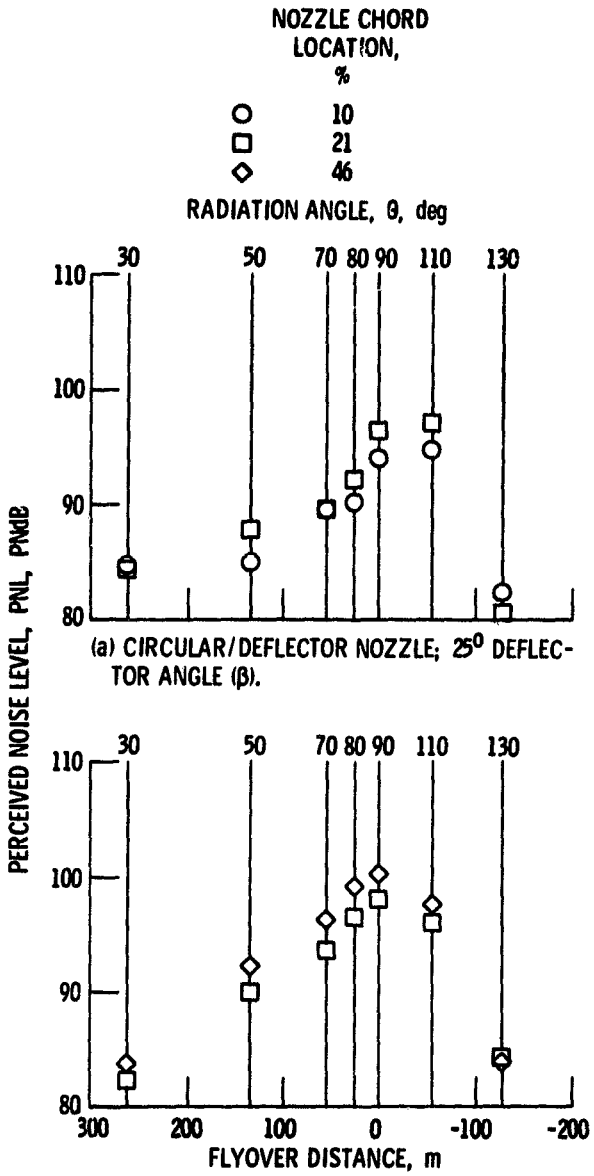

Figure 14. - Typical effect of nozzle chordwise location on PNL. Takeoff mode; nominal jet velocity, U_j, 260 m/sec; nozzle effective diam., D_{eff}, 66 cm.

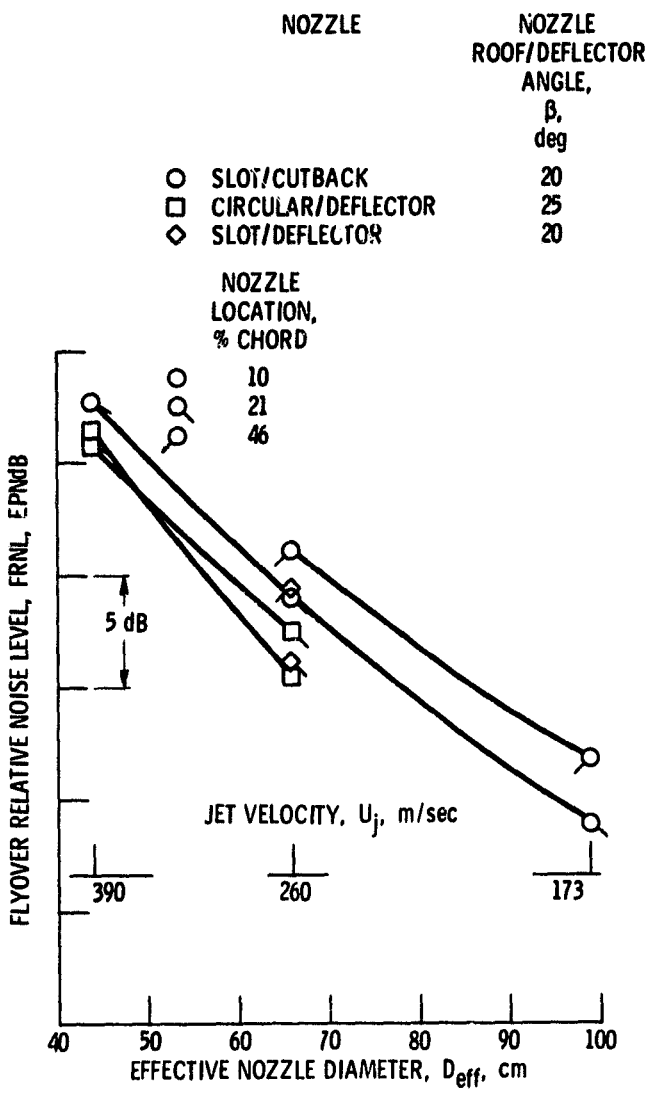

Figure 15. - Comparison of flyover relative noise levels as a function of effective nozzle size for takeoff mode.

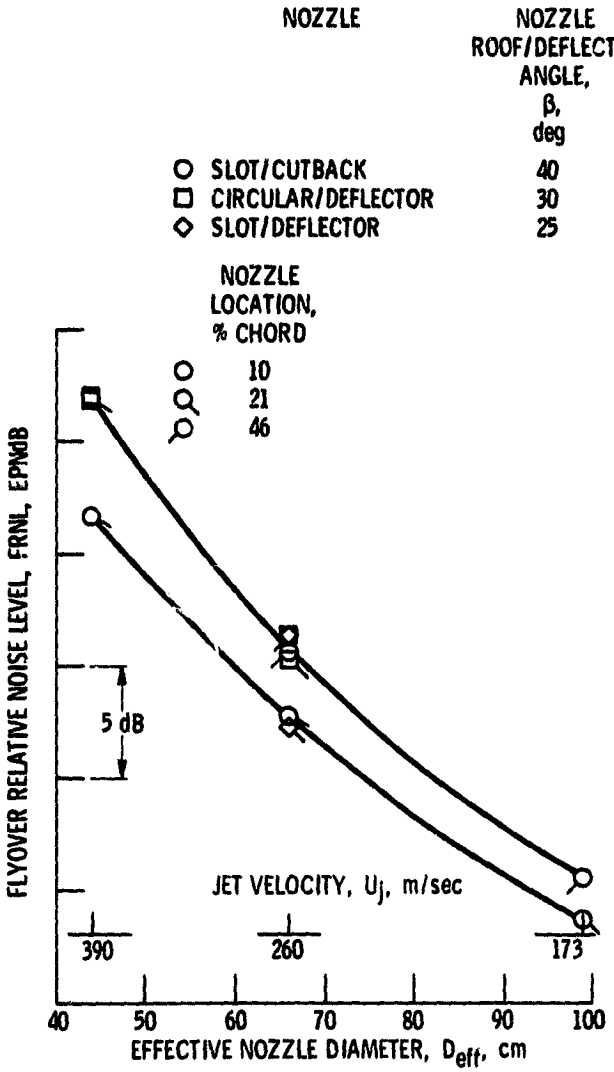

Figure 16. - Comparison of flyover relative noise levels as a function of effective nozzle size for approach mode.

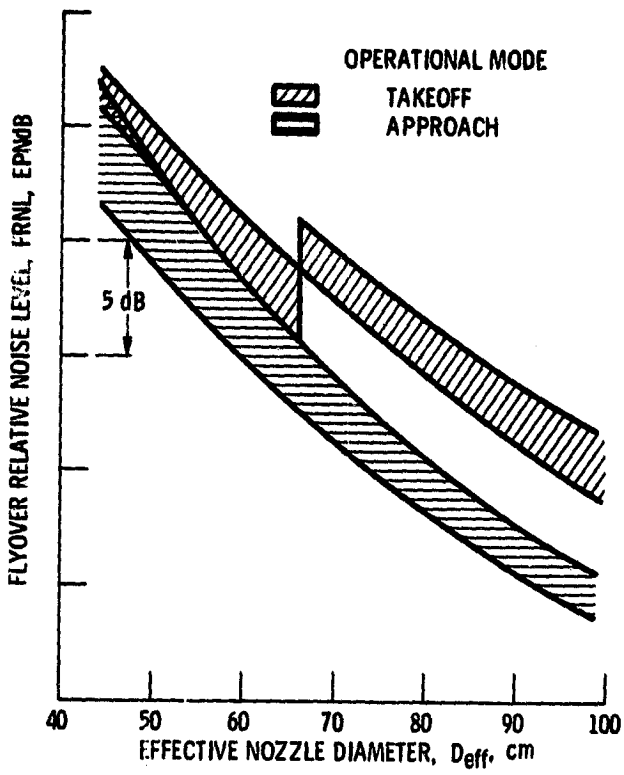

Figure 17. - Comparison of flyover relative noise levels for takeoff and approach modes.

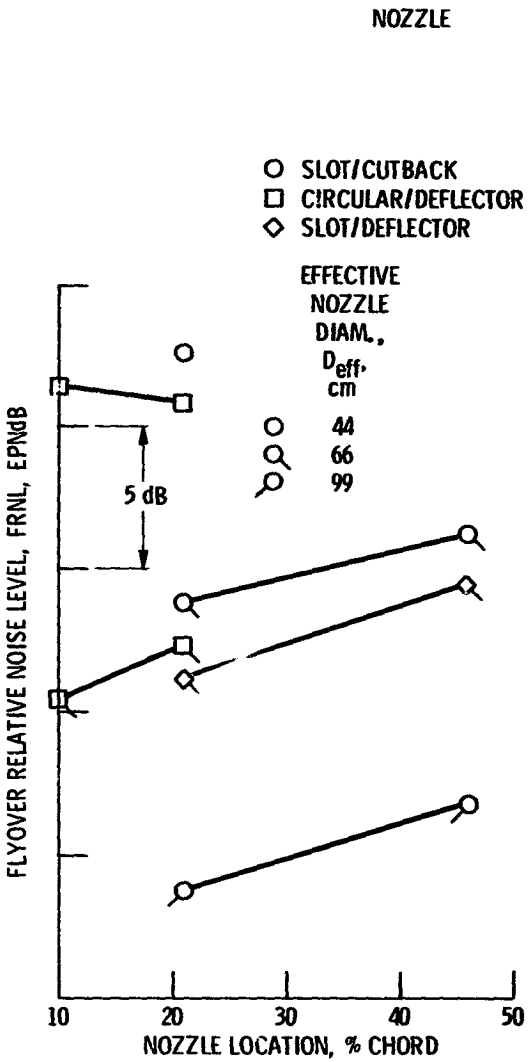

Figure 18. - Effect of nozzle chord location on flyover relative noise level for various nozzle configurations and sizes for takeoff mode.

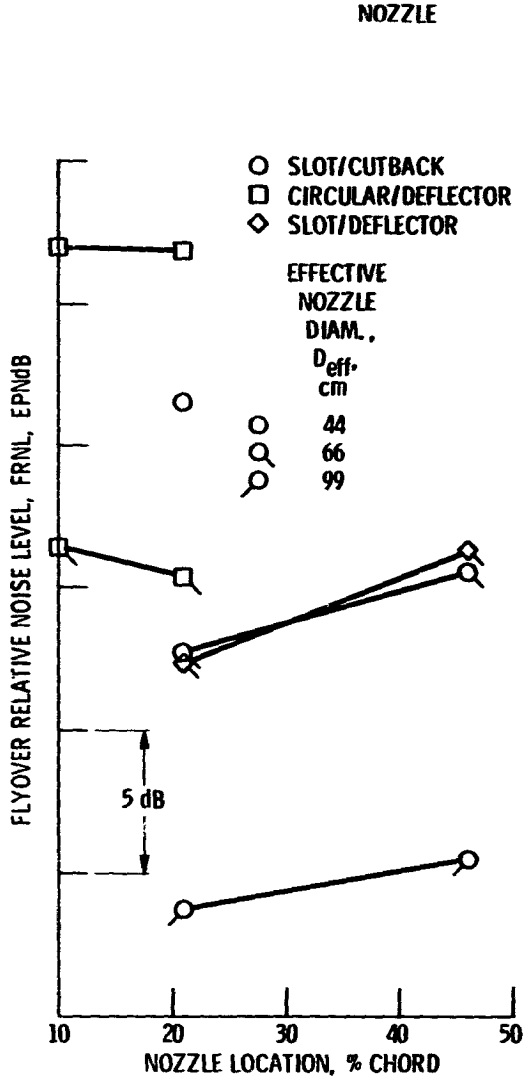

Figure 19. - Effect of nozzle chord location on flyover relative noise level for various nozzle configurations and sizes for approach mode.